

We are IntechOpen, the world's leading publisher of Open Access books Built by scientists, for scientists

6,900

Open access books available

186,000

International authors and editors

200M

Downloads

Our authors are among the

154

Countries delivered to

TOP 1%

most cited scientists

12.2%

Contributors from top 500 universities



WEB OF SCIENCE™

Selection of our books indexed in the Book Citation Index
in Web of Science™ Core Collection (BKCI)

Interested in publishing with us?
Contact book.department@intechopen.com

Numbers displayed above are based on latest data collected.
For more information visit www.intechopen.com



An Operational Statistical Scheme for Tropical Cyclone-Induced Rainfall Forecast

Qinglan Li , Hongping Lan , Johnny C.L. Chan ,
Chunyan Cao , Cheng Li and Xingbao Wang

Additional information is available at the end of the chapter

<http://dx.doi.org/10.5772/64859>

Abstract

Nonparametric methods are used in this study to analyze and predict short-term rainfall due to tropical cyclones (TCs) in a coastal meteorological station. All 427 TCs during 1953–2011, which made landfall along the Southeast China coast with a distance less than 700 km to a certain meteorological station, Shenzhen, are analyzed and grouped according to their landfalling direction, distance, and intensity. The corresponding daily rainfall records at Shenzhen Meteorological Station (SMS) during TCs landfalling period (a couple of days before and after TC landfall) are collected. The maximum daily rainfall (R24) and maximum 3-day accumulative rainfall (R72) records at SMS for each TC category are analyzed by a nonparametric statistical method, percentile estimation. The results are plotted by statistical boxplot, expressing in the probability of precipitation. The performance of the statistical boxplots was evaluated to forecast the short-term rainfall at SMS during the TC seasons in 2012 and 2013. The results show that the boxplot scheme can be used as a valuable reference to predict the short-term rainfall at SMS due to TCs landfalling along the Southeast China coast.

Keywords: tropical cyclone, rainfall forecast, nonparametric method, boxplot

1. Introduction

Tropical cyclones (TCs) are among the most destructive natural phenomena. TCs often bring about strong wind, heavy rainfall, and storm surge to the area along or close to the TCs' track. Among the three, heavy rainfall, which may lead to flash flooding and mudslides, is the most lethal natural disaster [1]. Typhoon Morakot, interacted with the strong southwest monsoon,

produced copious amounts of rainfall in Taiwan, with a record of 3031.5 mm during August 6–13, 2009 [2]. Hurricane Katrina, one of the deadliest hurricanes in the history of the United States, brought over 15 inches (381 mm) heavy rainfall to Florida at its landfall. The recorded maximum sustained wind speed reached 175 mph (280 km/h) and wind gusts reached 220 mph (350 km/h) at New Orleans, Louisiana [3]. Typhoon Morakot left 619 people dead and the death toll due to hurricane Katrina was over 1100 [3–5]. In order to alleviate enormous loss of lives and properties in the future, it is important to notice the local population and civil authorities to make appropriate preparation for the cyclones, including evacuation of the vulnerable areas where necessary. Accurate and timely (24 and 12 h before landfall) forecasting the TC track and the potential rainfall and wind induced by TC are vital and essential [6].

Most operational meteorologists rely heavily on numerical weather prediction (NWP) models in forecasting TCs. TC track forecasts have improved significantly over the past several decades [1, 7–9]. By contrast, the improvement in forecasting the TCs intensity has lagged behind the progress of TCs' track forecasting [9–12]. The capability for NWP models to predict short-term rainfall is still very limited [1, 6, 13, 14]. Quantitative forecasting of rainfall remains problematic and lags behind the TC's track forecast, although tropical cyclone forecasting is a successful enterprise with favorable benefit-to-cost returns [1]. Kidder et al. [6] report that because few observations are available while the storm is offshore, initializing numerical weather prediction models with sufficient details of the storm is impossible. Therefore, the rainfall forecasts by NWP models are not so accurate. The research of Xu et al. [15] shows that currently in China, there is no effective operational approach to forecast the heavy rainfall and wind induced by tropical cyclone. The forecast of the rainfall and wind due to TC in China all relies on NWP models and the experience of forecasters. Exploring other ways to predict short-term rainfall is therefore important and necessary.

When TCs approach the land or move across the coast, the TCs structure and intensity change greatly [16]. Landfalling TCs usually bring about heavy rainfall over land. Regarding the forecasting of rainfall due to a TC in a certain region (at a certain rain gauge), it is reported that the rainfall is associated with the distance from the TC center, TC intensity, TC track, TC moving velocity, and TC residing time, as well as the environmental background. Rainfall induced by a TC generally decreases exponentially with distance from the TC center [6, 17, 18]. With the same environmental background, the stronger the TC intensity, the heavier the precipitation will be [18]. The distribution of precipitation due to landfalling TC is asymmetric. In the Northern Hemisphere, the land on the right-hand side of TC would usually receive more intense and spatial rainfall than the land on the left-hand side [19], since the rain bands on the right would carry more moist oceanic air than those on the left. After landfall, the slower the moving speed of the TC or the longer the residence time for the TC in a certain region, the more opportunities and longer time will be for the TC to interact with other weather systems, which might lead to extreme rainfall accumulation [2].

The previous studies indicate that rainfall induced by a TC at a certain rain gauge is attributable to a variety of factors. However, most of those studies focused on either case studies or investigating a specific factor, and the conclusion is mostly qualitative. In this study, a statistical

scheme will be developed to forecast the maximum daily rainfall and 3-day accumulative rainfall at a meteorological station by considering the factor of distance between the station and the TC-landfalling center, the intensity of the TC, and the landfalling direction of the TC. This paper is arranged as follows. An overview of the data and methodology is presented in Section 2. Section 3 contains the description of the statistical boxplot scheme for TCs rainfall. The applications of the boxplot scheme to forecast the rainfall due to TCs in 2012 and 2013 are described in Section 4. Summaries and conclusions are given in the final section.

2. Data and methodology

This study focuses on Shenzhen to explore the potential rainfall caused by landfalling TCs. Shenzhen is a coastal and urban city in Guangdong Province, China [20–23], with the latitude from 22°27′ to 22°52′ and longitude from 113°46′ to 114°37′ (**Figure 1**). In summer and autumn, the city is often influenced by TCs. In this study, a total of 427 TCs, which made landfall along the Southeast China coast from 1953 to 2011 with the landfalling distance within 700 km to Shenzhen meteorological station (SMS), are studied.



Figure 1. Location of SMS; circles indicate region with radii of 100, 300, 500, and 700 km to SMS.

The records of daily rainfall from 1953 to 2011 in SMS are obtained from the Shenzhen Meteorological Bureau (SZMB). The maximum daily rainfall (from 20 pm of the previous day to 20 pm of the current day based on China standard time) and the maximum 3-day accumulative rainfall at SMS during the TC-landfalling period (within a couple of days before or after landfall) are computed. For example, if a TC makes landfall on date A, the rainfall at SMS on date A-2, A-1, A, A+1, and A+2 is collected as R_{A-2} , R_{A-1} , R_A , R_{A+1} , and R_{A+2} . The maximum daily rainfall (R24) and the maximum 3-day accumulative rainfall (R72) are computed as follows:

$$R24 = \text{maximum}(R_{A-2}, R_{A-1}, R_A, R_{A+1}, R_{A+2}) \quad (1)$$

$$R72 = \text{maximum}(R_{A-2}R_{A-1}R_A, R_{A-1}R_AR_{A+1}, R_AR_{A+1}R_{A+2}) \quad (2)$$

where $R_{A-2}R_{A-1}R_A$ refers to the accumulative rainfall on date A-2, A-1, A, etc.

TC characteristics from 1953 to 2011 are collected from China Meteorological Administration (CMA). The TC characteristics include the landfalling track, the distance between the TC-landfalling center and SMS, and the intensity (maximum wind speed near the TC center), which are proved to be strongly related to the rainfall caused by TCs in a certain region [6, 17–19].

As the rainfall distribution and intensity on the right side of TC track is different from those on the left side of TC track [19], all the TCs are first grouped into two categories: A, TCs landfalling to the west of SMS (landfalling longitude $<114^\circ\text{E}$); and B, TCs landfalling to the east of SMS (landfalling longitude $>114^\circ\text{E}$). Next, A and B are further grouped into seven categories according to the landfalling distance to SMS, for example, A1, within 100 km; A2, 100–200 km; A3, 200–300 km; ... A7, 600–700 km and B1, within 100 km; ... B7, 600–700 km. Finally, A1, A2, ..., B7 are grouped according to their landfalling intensity. According to the typhoon categorizing criterion of CMA (**Table 1**), there are six categories of TCs, which are super typhoon, severe typhoon, typhoon, severe tropical storm, tropical storm, and tropical depression. Among the 427 TCs, no landfalling TC was super typhoon. In this study, the TC intensity is stratified into three categories based on their respective TC-landfalling intensity scale (**Table 1**): TTY (total typhoon), which includes SuTY, STY, and TY; TTS (total tropical storm), which includes STS and TS; and TD. A1, A2, ..., B7 are therefore grouped into A1-TTY, A1-TTS, A1-TD, A2-TTY, A2-TTS, A2-TD, ..., B7-TTY, B7-TTS, and B7-TD. The flowchart of the TCs' categorizing steps is depicted in **Figure 2**.

| Category | Abbreviation | Sustained maximum winds near the center of TCs |
|-----------------------|--------------|--|
| Super typhoon | SuTY | ≥ 51 m/s |
| Severe typhoon | STY | 41.5–50.9 m/s |
| Typhoon | TY | 32.7–41.4 m/s |
| Severe tropical storm | STS | 24.5–32.6 m/s |
| Tropical storm | TS | 17.2–24.4 m/s |
| Tropical depression | TD | 10.8–17.1 m/s |

Table 1. Tropical Cyclone Intensity Scale according to CMA.

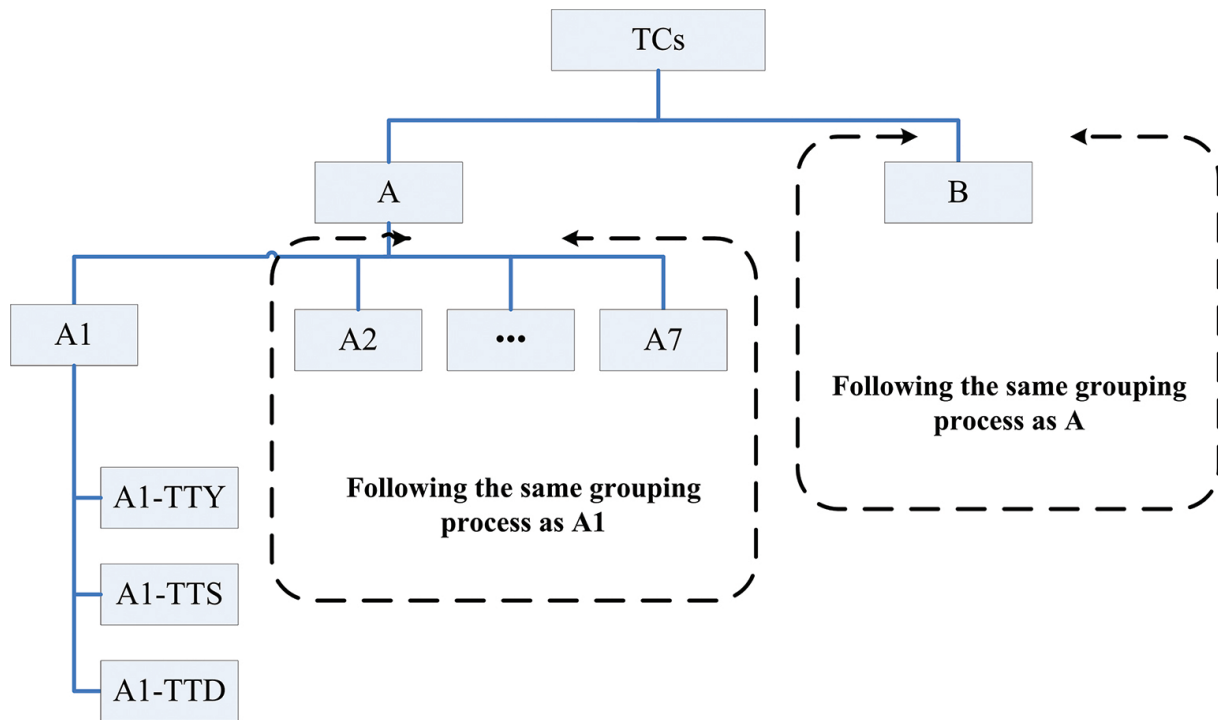


Figure 2. Flowchart of grouping process for landfalling tropical cyclone along the Southeast China coast.

Due to its nature of nonnormal distribution for precipitation [24], nonparametric method is a preferable approach to analyze typhoon-induced precipitation than parametric method [25]. A nonparametric statistical method, percentile estimation, is used to analyze the rainfall data in this study. Boxplots are applied to illustrate the analysis results. The detailed procedures are as follows:

Given n sorted rainfall observation $\{r_i\}$, $i = 1, \dots, n$, for a TC category, $0 < r_1 < r_2 < \dots < r_n$, the corresponding percentile for a rainfall record, r_i , is computed to be [26]

$$P_i = \frac{100}{n} \left(i - \frac{1}{2} \right) \quad (3)$$

When computing the rainfall of any percentile P , it needs to find two consecutive p_k and p_{k+1} , where $p_k < P < p_{k+1}$. The rainfall for this p percentile is therefore

$$r = r_k + \frac{P - p_k}{p_{k+1} - p_k} (r_{k+1} - r_k) \quad (4)$$

Using this approach, the 25th, 50th, and 75th percentile rainfall for each TC category can be computed. The analysis results are illustrated by a boxplot (**Figure 3**) to display the differences between sample populations [27]. There are five-number summaries for a boxplot: the lower

whisker (LW), lower quartile (Q1), median (Q2), upper quartile (Q3), and upper whisker (UW). Q1, Q2, and Q3 are the 25th, 50th, and 75th percentile of the population, respectively. Points are drawn as outliers if they are larger than $Q3 + 1.5 \times (Q3 - Q1)$ or smaller than $Q1 - 1.5 \times (Q3 - Q1)$. In **Figure 3**, two observations are considered as outliers, which are depicted by a red plus sign (+). The plotted whisker, UW (or LW) in the figure, is the maximum observation (or minimum observation), which is not an outlier.

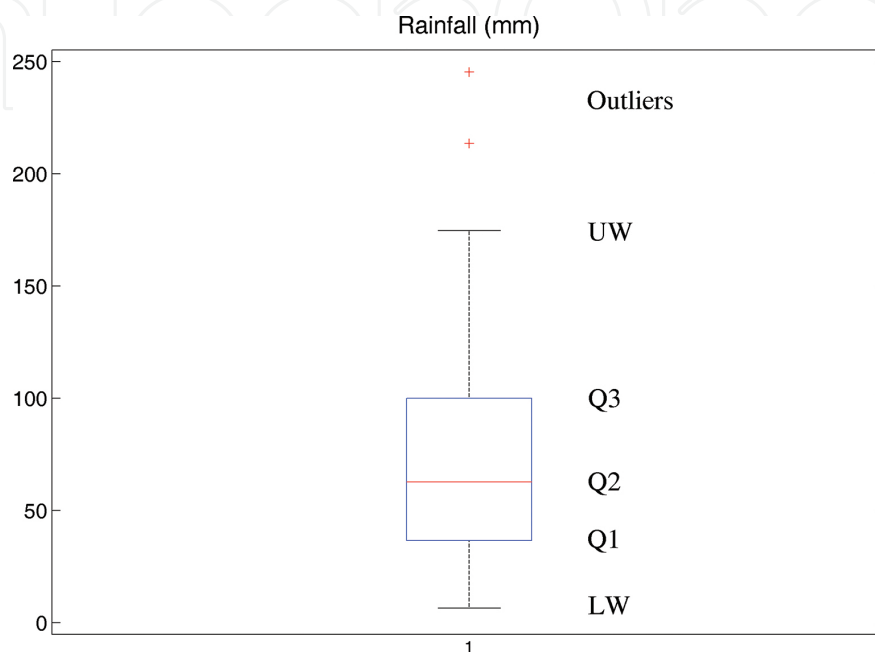


Figure 3. Boxplot as an example.

For practical use to forecast the rainfall due to a landfalling TC, the category of the landfalling TC is first determined based on the information of TC-landfalling distance to SMS from NWP models' forecast and the landfalling intensity from NWP models' forecast, as well as from the empirical experience of the forecasters. Then, referring to the boxplot corresponding to the landfalling TC category, the rainfall of R24 and R72 at the meteorological station can be estimated that the landfalling TC might cause the medium rainfall, 25–75% interquartile rainfall range, LW, UW, minimum rainfall, and maximum rainfall.

3. Statistical boxplots for TCs rainfall

Following the procedures mentioned in Section 2, all the historical TCs from 1953 to 2011, which made landfall within the distance of 700 km to SMS, are grouped into 42 categories. Because of the natural selection, it is impossible that each subgroup has approximately equal number of TCs. **Table 2** shows the groupings for TCs landfalling on the west of SMS, for example, "tms" in the table means the times of TCs for each category. For instance, there are 10 TTYs (2 severe typhoons and 8 typhoons) landfalling on the west of Shenzhen within 100

km distance to SMS (A1-TTY). The “tms” for other categories are from 4 to 29. For such small sample sizes, nonparametric statistics is seriously suggested to be suitable to analyze the datasets [25]. For each category of the TCs, the minimum, maximum, 25th percentile (Q1), 50th percentile (Q2), and 75th percentile (Q3) of the observed R24 and R72 are computed (Table 2).

| A | tms | R-24 (mm) | | | | | R-72 (mm) | | | | |
|--------|-----|-----------|-------|-------|-------|--------|-----------|-------|-------|--------|--------|
| | | Min | Max | Q1 | Q2 | Q3 | Min | Max | Q1 | Q2 | Q3 |
| A1-TTY | 10 | 93.7 | 247.4 | 120.3 | 152.1 | 226 | 102.1 | 347.9 | 185.8 | 263.1 | 290.8 |
| A1-TTS | 8 | 48.2 | 209.1 | 93.7 | 151.1 | 178.25 | 111.3 | 275.7 | 155 | 185.95 | 249.85 |
| A1-TD | 6 | 17.9 | 121.7 | 25.8 | 53.95 | 89.4 | 35.9 | 141.1 | 45.5 | 83.75 | 114.8 |
| A2-TTY | 4 | 101.1 | 213.5 | 114.5 | 140.1 | 182.9 | 138.2 | 478.5 | 154.1 | 235.3 | 389.55 |
| A2-TTS | 15 | 28.3 | 245.3 | 36.2 | 64.6 | 98.43 | 34.8 | 391.6 | 60.95 | 93.3 | 151.38 |
| A2-TD | 7 | 6.6 | 64.9 | 33.03 | 38 | 55.25 | 12.3 | 150.1 | 52.85 | 71.2 | 101.05 |
| A3-TTY | 6 | 23.5 | 80.9 | 41.1 | 60.9 | 80.3 | 35.4 | 131.8 | 58.5 | 98.35 | 114.3 |
| A3-TTS | 17 | 10.7 | 161 | 33.9 | 48.7 | 65.8 | 11.7 | 260 | 51.08 | 83.1 | 143.13 |
| A3-TD | 7 | 10.5 | 199.7 | 23.38 | 35.3 | 109.25 | 11.1 | 282.8 | 43.85 | 73.8 | 145.63 |
| A4-TTY | 6 | 41.9 | 73.4 | 54.7 | 62 | 68.2 | 42 | 128.2 | 71.3 | 84.4 | 90.4 |
| A4-TTS | 15 | 4.1 | 156.6 | 7.73 | 36.5 | 45.95 | 5.8 | 261.2 | 14.7 | 45.1 | 96.78 |
| A4-TD | 5 | 15.9 | 102.5 | 18.98 | 22.4 | 48.2 | 16.6 | 105.8 | 34.08 | 40.1 | 65.38 |
| A5-TTY | 22 | 6.1 | 115 | 15.4 | 35.9 | 54.7 | 6.7 | 246.3 | 24.7 | 60.05 | 91.3 |
| A5-TTS | 29 | 0.6 | 168.8 | 11.2 | 26.9 | 47.5 | 0.8 | 189.6 | 16.58 | 43.5 | 74.13 |
| A5-TD | 21 | 1 | 102 | 9.1 | 35.1 | 46.95 | 2.4 | 157.6 | 13.73 | 47.4 | 93.23 |
| A6-TTY | 12 | 0.5 | 91.4 | 10.2 | 22.3 | 35.1 | 0.5 | 140.8 | 17.3 | 35.55 | 48.85 |
| A6-TTS | 21 | 1.4 | 159.2 | 6.45 | 14.7 | 28.83 | 1.5 | 282.5 | 9.28 | 24.2 | 58.73 |
| A6-TD | 21 | 1.1 | 308.6 | 6.35 | 19.2 | 56.2 | 1.2 | 387.8 | 8.9 | 31.6 | 85.78 |
| A7-TTY | 10 | 0.1 | 45.5 | 1.9 | 11.95 | 21.4 | 0.1 | 64.9 | 2.4 | 17.55 | 38 |
| A7-TTS | 10 | 1.2 | 64.5 | 6.8 | 25.85 | 53.3 | 1.3 | 110.1 | 13.7 | 52.95 | 73.7 |
| A7-TD | 11 | 0.1 | 159.2 | 1.23 | 10 | 33.35 | 0.1 | 282.5 | 2.13 | 18.3 | 74.55 |

Table 2. Times of each TC category and the corresponding percentile for R-24 and R-72 for TCs landfalling on the west of SMS.

The boxplots of the historical rainfall records of R24 and R72 at SMS due to all the categories of TCs from 1953 to 2011 are plotted in Figure 4. Figure 4a and b are for the category TTY, (c and d) are for TTS and (e and f) are for TD. The thick vertical line in each of the subplots of Figure 4 refers to SMS. A7, A6, A5, A4, A3, A2, and A1 of the x-axis label refer to the TCs landfalling location, which are 600–700, 500–600, 400–500, 300–400, 200–300, 100–200 km, and within 100 km on the west of SMS. The meanings of B1, B2, ..., B7 are similar, but for the TCs landfalling on the east of SMS. Therefore, from Figure 4, the rainfall of R24 and R72 at SMS can be determined that each category of the landfalling TC might cause the 25–75% interquartile rainfall range, the lower whisker, upper whisker, minimum rainfall, and maximum rainfall.

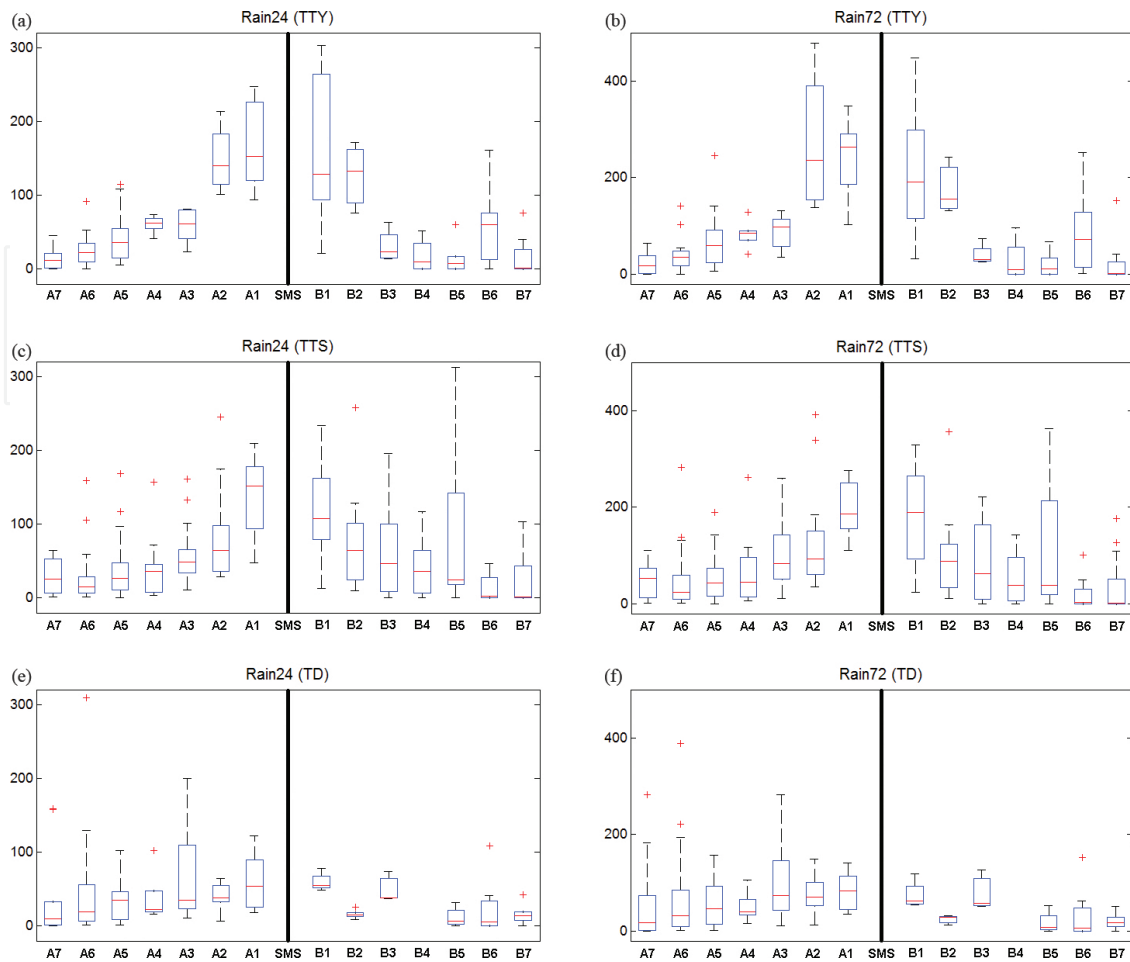


Figure 4. Boxplots for R24 and R72 rainfall at SMS from 1953 to 2011 due to TTYs (a and b), TTSs (c and d), and TDs (e and f). The vertical black thick line in the middle of each subplot denotes SMS. A on the x -label refers to the landfalling area, which is to the west of SMS, and B on the x -label refers to the landfalling area, which is to the east of SMS. The numbers after A and B on the x -label refer to the distance to SMS.

From **Figure 4**, it can be seen that the shape of the rainfall boxplots is not symmetric compared to the boxplots on the west and on the east of SMS. Generally, the TCs that make landfall on the west of SMS within the distance of 400 km would generally bring more rainfall to SMS than those TCs that make landfall on the east of SMS with similar landfalling intensity and distance. The median (Q2) records of R24 and R72 for TTY and TTS (**Figure 4a–d**) generally decrease with the increase of the landfalling distance to SMS, especially for TCs landfalling on the west of SMS. However, when the landfalling distance is outside 400 km, Q2 does not decrease as clearly as its change within 400 km. From **Figure 4a–d**, it can be seen that TCs that make landfall at B5 (with the distance of 400–500 km on the east of SMS) and B6 (with the distance of 500–600 km on the east of SMS) sometimes might cause very heavy rainfall at SMS. The reason might be that after those TCs land at B5–B6, they do not dissipate soon and continue to move west or east. During their continuous movement, they will probably interact with other weather system, such as southwesterly monsoon and mid-latitude trough, and bring plenty of moisture and energy over Southeast China. If SMS is on the passageway or near the passageway to transport such moisture and energy, heavy rainfall would occur in Shenzhen.

In addition from **Figure 4**, the variation of rainfall due to TDs does not change with distance as clearly as rainfall due to other categories of TCs. Furthermore, it can be seen from the figure that within the distance of 200 km, the median of the rainfall records (Q_2) is generally larger when the strength of the TCs is higher (i.e., $Q_{2\text{TTY}} > Q_{2\text{TTS}} > Q_{2\text{TD}}$). However, when outside 200 km, this pattern might change. For example, rainfall at SMS due to TTSs and TDs, which make landfall at B3, is even higher than rainfall due to TTYs landfalling at B3. TTSs that make landfall at B5 (more than 400 km away from SMS) might sometimes induce very large rainfall at SMS (**Figure 4c, d**), compared to TTYs that make landfall at the B5. This might be due to the influence of other factors, such as TC track, TC-moving velocity after landfalling, and the environmental background.

4. 2012, 2013 cases: forecasting and discussion

To apply the statistical boxplot scheme to forecast the potential maximum R24 and R72 rainfall due to a landfalling TC, the TC-landfalling location and intensity need to be identified first. Nowadays, operational forecasting models can usually predict the TC's track well, especially the track within 24 h [15]. Compared to the track forecast, the TC intensity forecast by NWP models is not so accurate at present. However, with the real-time observations from satellite and radar, forecasters have the ability to predict the intensity of the landfalling TC 12 h before TC landfall by rule of thumb, as it usually takes at least 12 h for a TC to change intensity or motion appreciably [1]. With the approximate TC-landfalling location and intensity available 12 h before the TC landfall, the statistical boxplot scheme can be then applied to forecast the rainfall of R24 and R72 at SMS.

In this section, the TCs that made landfall along the Southeast China coast in 2012 and 2013 will be used to test the performance of the boxplot scheme. In the typhoon seasons of these 2 years, there are 11 TCs landfalling within the distance of 700 km to SMS along the Southeast China coast. The detailed TC information is summarized in **Table 3**.

Based on the latest forecast for these 11 TCs' landfalling direction, location, and intensity, the boxplots for the corresponding TC categories are picked out. **Figure 5** shows these boxplots for the rainfall of R24, as well as the real maximum daily rainfall observation at SMS (black thick solid horizontal line) during the TC-landfalling period (rainfall within a couple of days before and after TC landfalling) due to these TCs. By comparison, the latest rainfall forecasts (brown solid horizontal line) before the TCs' landfall by European Center for Medium-Range Weather Forecasts (ECMWF) are plotted in **Figure 5** as well. ECMWF is renowned worldwide for providing the most accurate medium-range global weather forecasts up to 10 days ahead, monthly forecasts, and seasonal outlooks to 6 months ahead. It has been widely used for operational forecast and research purpose around the world [28–31]. ECMWF model is reported to well produce the medium-range forecasts of the Northwest Pacific subtropical high and South Asian high which have pronounced influences on the summertime persistent heavy rainfall in China [32]. The track of the TC in western Pacific and South China Sea is strongly affected by the area of the western Pacific subtropical high [33, 34]. Therefore, ECMWF's

forecasts of TC's track for the coming 12 and 24 h are usually reliable. SZMB has been relying on ECMWF for daily operational forecast since 2009. The finest resolution of ECMWF system used in SZMB is $0.125^\circ \times 0.125^\circ$. Xu et al. [28] reported that ECMWF model could provide valuable information for rainfall forecast up to the next 10 days; however, the ability for storm rainfall forecast was not reliable. For tropical cyclone forecast, ECMWF can usually accurately predict the TC's landfalling intensity and location by the latest forecast around 12 h before TC's landfall, but it cannot predict well the storm rainfall induced by TCs.

| Name | Landfalling time | Landfalling latitude ($^\circ\text{N}$) | Landfalling longitude ($^\circ\text{E}$) | Landfalling intensity | Distance (km) |
|---------|------------------|---|--|-----------------------|---------------|
| Doksuri | 6/30/03 | 22 | 113.2 | TTS | 102 |
| Vicente | 7/24/04 | 22 | 113 | TTY | 119 |
| Kai-Tak | 8/17/12 | 21 | 110.4 | TTY | 410 |
| TD1303 | 6/15/17 | 19.9 | 110.9 | TD | 436 |
| Bebinca | 6/22/11 | 19.2 | 110.7 | TTS | 506 |
| Rumbia | 7/02/06 | 21.1 | 110.2 | TTS | 424 |
| Cimaron | 7/18/22 | 24.1 | 117.9 | TTS | 434 |
| Jebi | 8/02/20 | 19.7 | 110.9 | TTS | 451 |
| Utor | 8/14/15 | 21.6 | 111.9 | TTY | 241 |
| Trami | 8/22/03 | 25.7 | 119.5 | TTY | 659 |
| Usagi | 9/22/20 | 22.7 | 115.4 | TTY | 263 |

Time format for landfalling time: month/day/hour; distance refers to the distance between the landfalling center of TC and SMS. The unit for latitude is degree north ($^\circ\text{N}$) and for longitude is degree east ($^\circ\text{E}$). The unit for distance is kilometer (km).

Table 3. Information about the 11 TCs landfalling within the distance of 700 km to SMS in 2012 (the first three TCs) and 2013 (the last eight TCs).

From **Figure 5**, it can be seen that the observed R24 rainfall records at SZMB for the 11 TCs are most of the time between the historical observed maximum and minimum rainfall for the corresponding category of landfalling TC, except for TY Trami and STY Usagi. TY Trami landed in Fujian province, China on August 22, 2013. It continued to move west to Jiangxi Province, until it finally disappeared in Hunan Province. During its process in mainland, Trami interacted with the strong southwest monsoon and brought immense downpours in Southeast China. It set a new rainfall record at Shenzhen for TTY category, which landed on the east of Shenzhen with the landfalling distance of 600–700 km. Similar condition is for STY Usagi. Usagi set a new rainfall record at Shenzhen for TTY category, which landed on the east of Shenzhen with the landfalling distance of 200–300 km. For the other TCs, most of the rainfall observations at SMS are within the interquartile range of the historical records (Q1–Q3), such as TS Doksuri, TY Vicente, TY Kai-Tak, TD1303, STS Rumbia, STS Jebi, and STY Utor, which are shown in

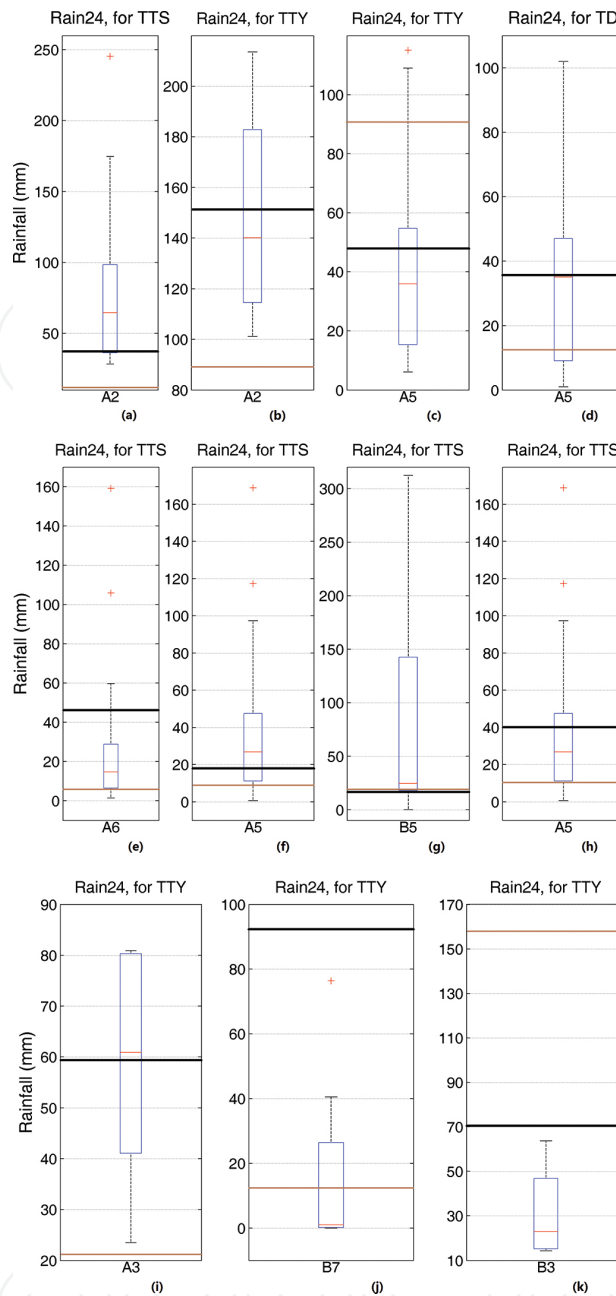


Figure 5. Comparison of the R24 rainfall forecasts for 11 TC cases in 2012 and 2013 by the boxplots and by ECMWF (brown solid horizontal line), as well as the real rainfall observation (black thick solid horizontal line): (a) for TS Dok-suri; (b) for TY Vicente; (c) for TY Kai-Tak; (d) for TD1303; (e) for TS Bebinca; (f) for STS Rumbia; (g) for STS Cimaron; (h) for STS Jebi; (i) for STY Utor; (j) for TY Trami; and (k) for STY Usagi.

Figure 5a–d,f,h,i, respectively. Similarly, more than 50% of R72 rainfall at SMS due to these TCs are within the interquartile range (Q1–Q3) of the historical records. By comparison, it can be seen that ECMWF by the latest model output can sometime accurately forecast the rainfall due to TCs, such as in **Figure 5f** and **g**. However, for the other cases, the discrepancies between the rainfall forecast by ECMWF and real rainfall observation at SMS are large. Therefore, besides the NWP, forecasters can use the historical rainfall observation boxplots (**Figure 4**) as a good reference to predict the potential short-term rainfall due to a landfalling TC.

The statistical boxplots scheme can provide valuable information to operational forecaster to predict the potential rainfall due to a TC. However, it must be known that there are still many uncertainties for the boxplots because of the small sample size for some TC categories due to the natural features, as well as the short observation history. With more TCs landfalling along the Southeast China coast in future, the larger will be the database of TCs and the more accurate will be for the short-term TC rainfall prediction by the boxplots scheme.

5. Conclusions

This study applied all the historical TCs landfalling along the Southeast China coast from 1953 to 2011 to explore a statistical boxplot scheme to forecast the maximum daily (R24) and 3-day accumulative rainfall (R72) at a certain rain gauge (SMS) during TC-landfalling period. Three TC's characteristics, including TC's landfalling direction, landfalling distance to SMS, and landfalling intensity, are considered to categorize all the historical TCs landfalling within the distance of 700 km to SMS. The corresponding historical daily rainfall records at SMS during the TC-landfalling period (rainfall within a couple of days before and after TC landfalling) are collected and organized according to the TC's category. The organized rainfall records for each TC category are analyzed by percentile estimation. The results are plotted in boxplots. It is concluded from the boxplots that the rainfall at a certain area is generally positively correlated to the intensity of the landfalling TC within 200-km distance to the landfalling center. Within the distance of 400 km to the landfalling location, the rainfall at SMS is generally negatively associated with the distance between TC's landfalling center and SMS. With the same intensity scale, TCs landfalling on the west of SMS will generally bring heavier rainfall at SMS than TCs landfalling on the east of SMS within the distance of 400 km. Eleven tropical cyclones landfalling within the distance of 700 km to SMS in 2012 and 2013 are used to evaluate the performance of the statistical boxplots to predict short-term rainfall at SMS. Results show that the boxplot scheme is very valuable to forecasters to provide rainfall range due to each TC category. For most of the time, the observed rainfall due to a landfalling TC is within the range of the historical rainfall records.

The boxplot scheme is easy to implement. The rainfall boxplots are quite helpful to operational forecasters. As of this writing, the technique is already in use as a valuable reference at SZMB to predict the short-term rainfall at SMS due to TCs.

Acknowledgements

This paper is supported by the Natural Science Foundation of Guangdong Province with Grant 2015A030313742, Special Fund for Science and Technology Development in Guangdong Province with Grant No. 2016A050503035, and The Innovation of Science and Technology Commission of Shenzhen Municipality with Grants JCYJ20120617115926138 and ZDSYS20140715153957030.

Author details

Qinglan Li^{1*}, Hongping Lan², Johnny C.L. Chan³, Chunyan Cao², Cheng Li² and Xingbao Wang^{1,4}

*Address all correspondence to: ql.li@siat.ac.cn

1 Shenzhen Institute of Advanced Technology, Chinese Academy of Sciences, Shenzhen, China

2 Shenzhen Meteorological Bureau, Shenzhen, China

3 School of Energy and Environment, City University of Hong Kong, Hong Kong, China

4 The Centre for Australian Weather and Climate Research, Bureau of Meteorology, Melbourne, VIC, Australia

References

- [1] Willoughby H.E., Rappaport E.N., Marks F.D. Hurricane Forecasting: The State of the Art. *Natural Hazards Review*. 2007; 8(3): 45–49.
- [2] Wu L., Liang J., Wu C. Monsoonal Influence on Typhoon Morakot (2009). Part I: Observational Analysis. *Journal of the Atmospheric Sciences*. 2011; 68: 2208–2221. DOI: <http://dx.doi.org/10.1175/2011JAS3730.1>.
- [3] Jonkman S.N., Maaskant B., Boyd E., Levitan M.L. Loss of life caused by the flooding of New Orleans after Hurricane Katrina: analysis of the relationship between flood characteristics and mortality. *Risk Analysis: An Official Publication of the Society for Risk Analysis*. 2009; 29(5): 678–98. DOI: 10.1111/j.1539-6924.2008.01190.x.
- [4] Cui P., Chen S., SU F., Zhang J. Formation and Mitigation Countermeasure of Geo-Hazards Caused by Moarc Typhoon in Taiwan. *Journal of Mountain Science*. 2010; 28(1): 103–115.
- [5] Knabb R.D, Rhome J.R., Brown D.P. National Hurricane Center. Tropical Cyclone Report: Hurricane Katrina, 23–30 August 2005 [Internet]. 20 December 2005 [Updated: 14 September 2011]. Available from: http://www.nhc.noaa.gov/data/tcr/AL122005_Katrina.pdf [Accessed: November 1, 2013].
- [6] Kidder S.Q., Kusselson S.J., Knaff J.A, Ferraro R.R, Kuligowski R.J., Turk M. The Tropical Rainfall Potential (TRaP) Technique. Part I: Description and Examples. *Weather and Forecasting*. 2005; 20(4): 456–464.

- [7] Aberson S.D. The Ensemble of Tropical Cyclone Track Forecasting Models in the North Atlantic Basin (1976–2000). *Bulletin of the American Meteorological Society*. 2001; 82(9): 1895–1904.
- [8] Franklin J.L., Mcadie C.J., Lawrence M.B. Trends in Track Forecasting for Tropical Cyclones Threatening the United States. *Bulletin of the American Meteorological Society*. 2003; 84(9): 1197–1203.
- [9] Rogers R., Aberson S., Black M., Black P., Cione J., Dodge P., et al. The Intensity Forecasting Experiment: A NOAA Multiyear Field Program for Improving Tropical Cyclone Intensity Forecasts. *Bulletin of the American Meteorological Society*. 2006; 87(11): 1523–1537.
- [10] DeMaria M., Gross J.M. Evolution of Tropical Cyclone Forecast Models. In: Simpson R., editor. *Hurricane! Coping with Disaster*. 1st ed. American Geophysical Union; 2003. p. 360. DOI: ISBN 0-87590-297-9.
- [11] Cecil D.J., Jones T.A., Knaff J.A., DeMaria M. Statistical Forecasting of Pacific and Indian Ocean Tropical Cyclone Intensity using 19-, 37-, and 85- GHz Brightness Temperatures. In: 26th Conference on Hurricanes and Tropical Meteorology; May 5, 2004; Miami, FL. American Meteorological Society; 2004. p. 302–303.
- [12] Knaff J.A., Sampson C.R., DeMaria M. An Operational Statistical Typhoon Intensity Prediction Scheme for the Western North Pacific. *Weather and Forecasting*. 2005; 20(4): 688–699.
- [13] Marchok T., Rogers R., Tuleya R. Validation Schemes for Tropical Cyclone Quantitative Precipitation Forecasts: Evaluation of Operational Models for U.S. Landfalling Cases. *Weather and Forecasting*. 2007; 22(4): 726–746.
- [14] Liu G., Chao C., Ho C. Applying Satellite-Estimated Storm Rotation Speed to Improve Typhoon Rainfall Potential Technique. *Weather and Forecasting*. 2008; 23(2): 259–269.
- [15] Xu Y.L., Zhang L., Gao S.Z. The Advances and Discussions on China Operational Typhoon Forecasting (in Chinese). *Meteorological Monthly*. 2010; 36(7): 43–49.
- [16] Chen L.S. Research Progress on the Structure and Intensity Change for the Landfalling Tropical Cyclones. *Journal of Tropical Meteorology*. 2012; 18(2): 113–118.
- [17] Simpson R.H., Riehl H. *The Hurricane and its Impact*. Louisiana State University Press, Baton Rouge; 1981. 398 p.
- [18] Pfof R.L. Operational Tropical Cyclone Quantitative Precipitation Forecasting. *National Weather Digest*. 2000; 24(1–2): 61–66.
- [19] Chan J.C.L., Liang X. Convective Asymmetries Associated with Tropical Cyclone Landfall. Part I: f -Plane Simulation. *Journal of the Atmospheric Sciences*. 2003; 60(13): 1560–1576.

- [20] Wang M.J., Zhang X.L., Li X.R. Analysis of Meteorological Conditions for the Base of Marine Sports in the 26th Summer Universiade in Shenzhen in 2011. *Journal of Tropical Meteorology*. 2011; 17(2): 187–192.
- [21] Zhang X.L., Li L., Du Y., Jiang Y., Fang X.Y., Li M., et al. A Numerical Study on the Influences of Urban Planning and Construction on the Summer Urban Heat Island in the Metropolis of Shenzhen. *Journal of Tropical Meteorology*. 2011; 17(4): 392–398.
- [22] Chen J., Li Q.L., Niu J., Sun L.Q. Regional Climate Change and Local Urbanization Effects on Weather Variables in Southeast China. *Stochastic Environmental Research and Risk Assessment*. 2011; 25(4): 555–565. DOI: 10.1007/s00477.
- [23] Li Q.L., Chen J. Teleconnection between ENSO and climate in South China. *Stochastic Environmental Research and Risk Assessment*. 2014; 28(4): 927–941. DOI: 10.1007/s00477-013-0793-z.
- [24] Turco M., Llasat M.C. Trends in Indices of Daily Precipitation Extreme in Catalonia (NE Spain), 1951-2003. *Natural Hazards and Earth System Sciences*. 2011; 11: 3213–3226.
- [25] Pett M.A. *Nonparametric Statistics for Health Care Research – Statistics for Small Samples and Unusual Distributions*. 1st ed. Thousand Oaks: Sage Publications; 1997. 307 p.
- [26] Stark H., Woods J. *Probability, Statistics, and Random Processes for Engineers*. 4th ed. Boston: Pearson; 2012. 704 p.
- [27] McGill R., Tukey J.W., Larsen W.A. Variations of Box Plots. *Journal of the American Statistical Association*. 1978; 32(1): 12–16.
- [28] Xu W.W., Chen S.P., Li Q.L. Evaluation of Precipitation Forecast in Shenzhen for the First Raining Season in 2012 by ECMWF model and HAPS model (in Chinese). *Guangdong Meteorology*. 2013; 35(5): 6–9.
- [29] Halperin D.J., Fuelberg H.E., Hart R.E., Cossuth J.H., Sura P. An Evaluation of Tropical Cyclone Genesis Forecasts from Global Numerical Models. *Weather and Forecasting*. 2013; 28(6): 1423–1445. DOI: <http://dx.doi.org/10.1175/WAF-D-13-00008.1>.
- [30] Wang Y., Bellus M., Geleyn J.F., Ma X.L., Tian W.H., Weidle F. A New Method for Generating Initial Condition Perturbations in a Regional Ensemble Prediction System: Blending. *Monthly Weather Review*. 2014; 142(5): 2043–2059.
- [31] Magnusson L., Bidlot J.R., Lang S.T.K., Thorpe A., Wedi N. Evaluation of Medium-Range Forecasts for Hurricane Sandy. *Monthly Weather Review*. 2014; 142(5): 1962–1981.
- [32] Niu R.Y., Zhai P.M. Synoptic Verification of Medium-Extended-Range Forecasts of the Northwest Pacific Subtropical High and South Asian High Based on Multi-Center TIGGE Data. *Acta Meteorologica Sinica*. 2013; 27(5): 725–741.

- [33] Sun Y., Zhong Z., Lu W., Hu Y.J. Why Are Tropical Cyclone Tracks over the Western North Pacific Sensitive to the Cumulus Parameterization Scheme in Regional Climate Modeling? A Case Study for Megi (2010). *Monthly Weather Review*. 2014; 142(3): 1240–1249.
- [34] Tao L., Li S.J. Impact of Tropical Intraseasonal Oscillation on the Tracks of Tropical Cyclones in the Western North Pacific. *Journal of Tropical Meteorology*. 2014; 20(1): 26–34.

IntechOpen

IntechOpen